Percolation model for electron conduction in films of metal nanoparticles linked by organic molecules

K.-H. Müller,* J. Herrmann, B. Raguse, G. Baxter, and T. Reda
Commonwealth Scientific and Industrial Research Organization, Telecommunications and Industrial Physics, Sydney 2070, Australia
(Received 10 April 2002; published 26 August 2002)

We have investigated theoretically and experimentally the temperature dependence of the conductance of films of Au nanoparticles linked by alkane dithiol molecules in the temperature range between 5 and 300 K. Conduction in these films is due to tunneling of single electrons between neighboring metal nanoparticles via the linker molecules. During tunneling an electron has to overcome the Coulomb charging energy. We find that the observed temperature dependence of the conductance is non-Arrhenius-like and can be described in terms of a percolation theory which takes account of disorder in the system. Disorder in our nanoparticle films is caused by variations in the nanoparticle size, fluctuations in the separation gaps between adjacent nanoparticles and by offset charges. To explain in detail our experimental data, a wide distribution of separation gaps and charging energies has to be assumed. We find that a wide Coulomb charging energy distribution can arise from random offset charges even if the nanoparticle size distribution is narrow.

DOI: 10.1103/PhysRevB.66.075417 PACS number(s): 73.63.−b, 73.23.Hk, 72.80.Ng, 81.07.Pr

I. INTRODUCTION

Several attempts have been made to understand electron transport in assemblies of metal nanoparticles linked by organic molecules.[1,2] However, despite of these studies, several aspects of the electron transport mechanism in nanoparticle assemblies are still poorly understood. With nanoparticle arrays as ''artificial solids''[3] expected to provide useful model systems for the study of correlated electrons and as potential building blocks for nanoelectronics, a thorough understanding of metal nanoparticle assemblies is essential. Describing in detail the electron transport mechanism in realistic assemblies becomes intricate because of the inherent strong disorder present in most nanoparticle assemblies. One can distinguish three kinds of disorder. First, the overall global structural disorder in the topology of the assembly; secondly, local structural disorder due to particle size variations and fluctuations in the separation gap between adjacent nanoparticles; and thirdly, local charge disorder due to random immobile offset charges induced by trapped impurity charges in the substrate and possibly in the linker molecules. The effect of certain types of disorder on the conductance of metal nanoparticles has been investigated using Monte Carlo simulations on one-dimensional and two-dimensional arrays of nanoparticles.[4–8] In these simulations disorder was incorporated by taking account of random offset charges as well as variations in the particle size and the capacitative coupling between adjacent nanoparticles.

Because previous experimental work on the temperature dependence of the conductance $G(T)$ could not clearly distinguish between $\ln G \sim T^{-1}$ and $\sim T^{-1/2}$ behavior,[2] the emphasis of our paper is to investigate in detail theoretically and experimentally the temperature dependence of the conductance of alkane dithiol linked 3D nanoparticle films. Due to the disorder in our samples we treat the films as conductor networks of widely varying tunnel conductances which locally connect adjacent nanoparticles and apply percolation theory to estimate the temperature dependence of the film conductance. While Monte Carlo simulations can only be performed on assemblies of relatively small size, percolation theory can satisfactorily describe assemblies consisting of large numbers of nanoparticles as in the case of our nanoparticle films.

In Sec. II we develop a theoretical model for the electron conduction in a disordered nanoparticle film. Strong disorder in our films allows us to employ percolation theory. For the case of low temperature and small applied voltages we derive a simple analytical expression for the film conductance G_{tot} where we find $\ln(G_{\mathrm{tot}}/G_0) \sim T^{-1/2}$. In Sec. III we describe the preparation of our nanoparticle films and report on the experimental procedure used to measure the temperature dependence of G_{tot}. Section IV discusses and compares our experimental and theoretical results. Finally in Sec. V we show that wide distributions for the Coulomb charging energies and the nanoparticle separation gaps can be expected in our films.

II. THEORY

In order to develop formulas for the conductance of a nanoparticle film we first consider two neighboring normal-metal nanoparticles with electrostatic potential difference V. The nanoparticles are separated by a gap L formed by organic linker molecules which surround the nanoparticles (see Fig. 1). Using scattering theory, the electron current I which flows between the two metal nanoparticles is given by[9]

$$I = \frac{4\pi e}{\hbar} \sum_{r,l} \{ f(E_l - eV)[1 - f(E_r - E_c)] - f(E_r)[1 - f(E_l - eV - E_c)] \} |T_{lr}|^2 \delta(E_r - E_l). \quad (1)$$

Here e is the electron charge and the sum is over all the single electron states l and r of the left and right nanoparticle, respectively. The function f is the Fermi-Dirac distribution $f(x) = (1 + e^{(x - E_F)/kT})^{-1}$, where T is the temperature and E_F the Fermi energy of the electrons in the metal nano-

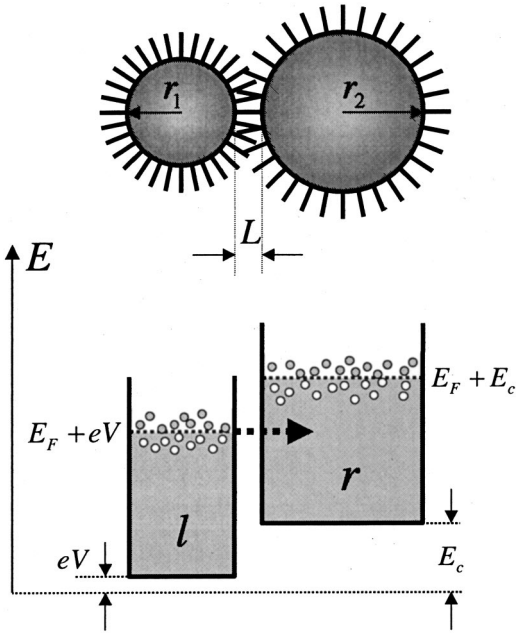

FIG. 1. Schematic energy diagram of two neighboring metal nanoparticles with separation gap L. The electrons in the normal-metal nanoparticles are described in terms of free Fermi gases. The electrostatic potential between the nanoparticles is eV. When an electron tunnels from the left (l) to the right (r) nanoparticle it has to overcome the Coulomb charging energy E_c.

particles. The quantities T_{lr} are the transition matrix elements and E_l and E_r are the energy levels of electrons in the nanoparticles. E_c is the Coulomb charging energy (Coulomb blockade energy) required to move an electron from one nanoparticle to a neighboring one. In our case the nanoparticles are 8 nm in diameter and therefore the electron level spacing is negligibly small. Figure 1 shows an energy diagram illustrating the transition of an electron moving from the left (l) metal nanoparticle to its neighbor nanoparticle on the right (r). Because, in our case, $eV \ll E_F$ as well as $E_c \ll E_F$, Eq. (1) can be written in the form

$$I = \frac{4\pi e}{\hbar}|T(E_F)|^2\rho^2(E_F)\int_{-\infty}^{\infty} dE\{f(E-eV)[1-f(E-E_c)] - f(E)[1-f(E-eV-E_c)]\}. \quad (2)$$

Here, $\rho(E_F)$ is the electron density of states at the Fermi level. The factor 4 includes the spin degeneracy. In Eq. (2), the E integration has been extended to negative values $(-\infty)$ which is possible because $kT \ll E_F$, allowing the integral in Eq. (2) to be evaluated analytically resulting in[10]

$$I = \frac{4\pi e}{\hbar}|T(E_F)|^2\rho^2(E_F)\left[\frac{E_c+eV}{1-e^{(E_c+eV)/kT}} - \frac{E_c-eV}{1-e^{(E_c-eV)/kT}}\right]. \quad (3)$$

Since we only consider electrical conduction in nanoparticle films for small applied voltages where $eV \ll E_c$, Eq. (3) becomes

$$I = \frac{8\pi e^2}{\hbar}|T(E_F)|^2\rho^2(E_F)\frac{1-(1-E_c/kT)e^{E_c/kT}}{(1-e^{E_c/kT})^2}V. \quad (4)$$

Equation (3) is equivalent to the results obtained from the so-called orthodox theory of single-electron tunneling[11] which is valid if the resistance R_T of all the tunnel barriers in the system is much greater than the quantum resistance $R_Q = h/e^2 \simeq 26\ \mathrm{k}\Omega$.

Assuming a simple tight-binding model to describe alkane dithiol linker molecules one obtains in the weak coupling limit using T-matrix theory[12]

$$|T(E_F)|^2 = \left|\frac{V_{l1}V_{Nr}}{V_B}\right|^2\left(\frac{V_B}{E_B-E_F}\right)^{2N}, \quad (5)$$

where N is the number of carbon and sulphur atoms in the alkane dithiol molecule, V_{l1} and V_{Nr} are matrix elements describing the interaction of the left nanoparticle with the first sulphur atom (1) and the right nanoparticle with the last sulphur atom (N). V_B is the matrix element of the tight binding interaction of neighboring atom sites while E_B is the approximate energy level of the lowest unoccupied local electron orbitals on the chain of sulphur and carbon atoms. The gap L between nanoparticles is determined by the length of the organic linker molecule which is $L = a_0(N+1)$ where a_0 is the average distance (along a straight line) between the carbon and sulphur atoms. Thus

$$|T(E_F)|^2 \sim e^{-\beta L}, \quad (6)$$

where

$$\beta = \frac{2}{a_o}\ln\frac{E_B-E_F}{V_B}. \quad (7)$$

More elaborate calculations which do not assume weak coupling lead to a similar exponential L dependence of $|T(E_F)|^2$ as in Eq. (6).[13] Instead of the tight-binding model approach one could also attempt to estimate $|T(E_F)|^2$ using the simple WKB method[9] for a tunnel barrier of constant height U_0. This also leads to an exponential drop of $|T(E_F)|^2$ with L, i.e.,

$$|T(E_F)|^2 \sim e^{-\beta' L}, \quad (8)$$

where

$$\beta' = (8mU_0/\hbar^2)^{1/2}. \quad (9)$$

Here, m is the effective mass of the electrons in the nanoparticles. From Eqs. (4) and (6) [or (8)] it follows that

$$I \sim e^{-[\beta L + g(E_c/kT)]}V, \quad (10)$$

where

$$g(E_c/kT) = -\ln\frac{1-(1-E_c/kT)e^{E_c/kT}}{(1-e^{E_c/kT})^2}. \quad (11)$$

In a nanoparticle film, adjacent nanoparticles can thus be viewed as being connected by local conductances G where

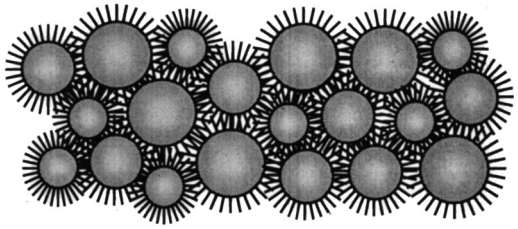

FIG. 2. Schematic view of part of a disordered film of nanoparticles linked by organic molecules.

$$G \sim e^{-\xi} \tag{12}$$

and

$$\xi = \beta L + g(E_c/kT). \tag{13}$$

Instead of trying to estimate the value of β using Eqs. (7) or (9), we take β from measurements on self-assembled monolayers of alkane dithiols assuming that the molecules have a tilt angle of 30° relative to a (111) gold surface. We use the result of Ref. 14, i.e., $\beta = 12.875\ \text{nm}^{-1}$. This value is similar to other β values found in the literature.[15]

Our nanoparticle films are disordered due to spatial variations in the separation gap L as well as variations in the Coulomb charging energy E_c. Disorder in L is caused by nanoparticle size fluctuations and by possible fluctuations in the linker-molecule concentration during film assembly. Disorder in the charging energy E_c is partly caused by nanoparticle size fluctuation but possibly most strongly by offset charge disorder. Figure 2 illustrates local structural disorder in a nanoparticle assembly due to particle size variations and fluctuations in the separation gaps. Our experimental results, discussed in detail later, indicate that ξ [Eq. (13)] typically varies from 5 to 50 where the variational range is largest at the lowest temperature. Such a strongly disordered nanoparticle film can thus be viewed as a network of widely varying conductors which can be well described in terms of percolation theory.[16–18]

In percolation theory, the total conductance G_{tot} of a highly disordered conductor network is given by

$$G_{\text{tot}} = G_0 e^{-\xi_c}. \tag{14}$$

Here, ξ_c is the value of ξ at the percolation threshold, which is the point where, in a thought experiment, an infinitely large connected cluster starts to emerge when randomly chosen pairs of neighboring nanoparticles are connected by conductors in a descending order of G values. In the following, we are not attempting to estimate the analytical form of the temperature independent prefactor G_0 of Eq. (14), but instead investigate the temperature dependence of ξ_c. Denoting by f_c the fraction of conductors G which are in place at the percolation threshold and by $P(\xi)$ the probability density to find a pair of neighboring nanoparticles with conductance $G \sim e^{-\xi}$ in the film, ξ_c can be determined from the equation

$$f_c = \int_0^{\xi_c} P(\xi) d\xi. \tag{15}$$

For a densely packed, three-dimensional lattice of nanoparticles we take $f_c = 0.119$ which is the bond percolation threshold of an fcc lattice.[19] As will become clear later, one can assume that L and E_c are uncorrelated, and thus one can write

$$P(\xi) = (1 - f_v) \int P_\lambda(\lambda) P_\epsilon(\epsilon) \delta[\xi - \lambda - g(\epsilon)] d\lambda\, d\epsilon, \tag{16}$$

where f_v is the fraction of voids and $P_\lambda(\lambda)$ and $P_\epsilon(\epsilon)$ are the probability densities of the occurence of a pair of neighboring nanoparticles in the film with separation gap L and Coulomb energy E_c where we have introduced the abbreviations

$$\lambda = \beta L \quad \text{and} \quad \epsilon = E_c/kT. \tag{17}$$

The δ function in Eq. (16) takes account of the constraint $\xi = \lambda + g(\epsilon)$ [Eq. (13)]. Finally, from Eqs. (15) and (16) one obtains the equation

$$\frac{f_c}{1 - f_v} = \int_0^\infty d\epsilon\, P_\epsilon(\epsilon) \int_0^{\xi_c} d\xi\, P_\lambda[\xi - g(\epsilon)]. \tag{18}$$

Equation (18) is the key equation of our investigation. Since the exact forms of $P_\lambda(\lambda)$ and $P_\epsilon(\epsilon)$ are not known, we choose for simplicity square distributions where

$$P_\lambda = \begin{cases} \dfrac{1}{\Delta\lambda} & \text{for } \lambda_M - \Delta\lambda/2 \leqslant \lambda \leqslant \lambda_M + \Delta\lambda/2, \\ 0 & \text{otherwise,} \end{cases} \tag{19}$$

and

$$P_\epsilon = \begin{cases} \dfrac{1}{\Delta\epsilon} & \text{for } \epsilon_M - \Delta\epsilon/2 \leqslant \epsilon \leqslant \epsilon_M + \Delta\epsilon/2, \\ 0 & \text{otherwise.} \end{cases} \tag{20}$$

Here, $\lambda_M = \beta L_M$ and $\epsilon_M = E_{cM}/kT$ are the mean values of the distributions where L_M is the average gap (excluding voids) separating neighboring nanoparticles and E_{cM} is the average Coulomb charging energy. $\Delta\lambda$ and $\Delta\epsilon$ are the widths of the distributions.

For E_{cM} we use a formula derived by Abeles *et al.*,[20] i.e.,

$$E_{cM} = \frac{e^2}{8\pi\epsilon_0\epsilon_r} \frac{L_M}{r_M(r_M + L_M)}. \tag{21}$$

Here, ϵ_0 is the vacuum permittivity and ϵ_r the relative permittivity of the molecules surrounding the nanoparticles, and r_M is the average radius of the nanoparticles.

At low temperatures, Eq. (11) can be approximated by

$$g(E_c/kT) \simeq -\ln\left[\frac{E_c}{kT} e^{-E_c/kT}\right]. \tag{22}$$

Ignoring the weak E_c/kT dependence of the prefactor, one obtains

$$g(E_c/kT) \simeq \frac{E_c}{kT}. \tag{23}$$

Using Eq. (23), the key Eq. (18) can be evaluated analytically. For $\Delta\epsilon \geqslant \Delta\lambda$ one derives

$$\xi_c = \begin{cases} \left(\dfrac{2f_c\Delta\lambda\Delta\epsilon}{1-f_v}\right)^{1/2} + \lambda_M - \Delta\lambda/2 + \epsilon_M - \Delta\epsilon/2 & \text{if } -\Delta\lambda/2 \leqslant \xi_c - \lambda_M - \epsilon_M + \Delta\epsilon/2 \leqslant \Delta\lambda/2, \\ \lambda_M + \epsilon_M - \left(\dfrac{1}{2} - \dfrac{f_c}{1-f_v}\right)\Delta\epsilon & \text{if } \Delta\lambda/2 - \Delta\epsilon/2 \leqslant \xi_M - \lambda_M - \epsilon_M \leqslant \Delta\epsilon/2 - \Delta\lambda/2. \end{cases} \tag{24}$$

The expression for ξ_c when $\Delta\epsilon < \Delta\lambda$ is obtained by exchanging the symbols ϵ and λ in Eq. (24). As can be seen from Eq. (24), if the P_λ and P_ϵ distributions are wide, i.e., $\Delta\epsilon = 2\epsilon_M$ and $\Delta\lambda = 2\lambda_M$, then

$$\xi_c = \left(\frac{2f_c\Delta\lambda\Delta\epsilon}{1-f_v}\right)^{1/2}, \tag{25}$$

i.e.,

$$\xi_c = \left(\frac{8f_c\beta L_M E_{cM}}{(1-f_v)kT}\right)^{1/2} \sim T^{-1/2}, \tag{26}$$

which is valid over a wide temperature range. For $\Delta\lambda \to 0$, one obtains

$$\xi_c = \frac{f_c\Delta\epsilon}{1-f_v} + \lambda_M, \tag{27}$$

and thus $\xi_c \sim T^{-1} + \text{const}$, meaning that using the approximate expression Eq. (23) for $g(E_c/kT)$, G_{tot} shows Arrhenius behavior if the P_λ distribution is narrow independent of the width of the P_ϵ distribution.

III. EXPERIMENT

The preparation of our nanoparticle film samples is described in detail elsewhere.[21] Briefly, a toluene solution of tetraoctylammonium bromide-coated Au nanoparticles with average diameters of 8 nm was produced using the method of Brust *et al.*[22,23] The nanoparticle films were fabricated in a two step procedure: In the first step, the solution of Au nanoparticles is treated with a solution of α,ω-alkane dithiol to cause the nanoparticles to cross link via the α,ω-alkane dithiol molecules, forming nanoparticle aggregates. In the second step, these nanoparticle aggregates are vacuum filtered through a nanoporous support.

We have found that by allowing the aggregation of the nanoparticles to proceed for only a limited time (i.e., before precipitation occurs) and by filtering the material through a nanoporous filter medium a coherent, uniform film of nanoparticle material is deposited onto the surface of the porous substrate that is not readily redispersible in solution. Once the solvent has dried, nanoparticle films are formed that are robust, can readily be handled and flexed without delamination from the substrate and are quite resistant to touch. The thickness of the film can be varied by adjusting the volume of cross-linked nanoparticle solution filtered through the nanoporous support.

We prepared films of nanoparticles of two different types of alkane dithiols, $HS(CH_2)_nSH$, where $n=2$ and $n=8$. For the nanoporous substrate, polyvinylidene fluoride (PVDF) filter membranes[24] were used. The typical thickness of our nanoparticle films was 0.3 μm as determined by atomic force microscopy.

For electrical conductance measurements, the films were cut into strips of about 10 mm length and 2 mm width. Electrical contacts spaced about 1 mm apart were made using conductive silver paste and gold wires. Conductance measurements in the temperature interval from 5 to 300 K were performed in a helium cryostat using a fixed excitation voltage of 5 V.

IV. RESULTS AND DISCUSSION

Figure 3 shows the calculated values of $G_{\text{tot}}/G_0 = e^{-\xi_c}$ versus $1/T$ for different choices of $\Delta\lambda$ and $\Delta\epsilon$ using the analytical expression for ξ_c of Eq. (24) which is based on the approximate expression Eq. (23). The mean separation between neighboring nanoparticles is $L_M = \lambda_M/\beta = 0.8$ nm which corresponds to the length of the $HS(CH_2)_2SH$ linker molecule. The mean charging energy E_{cM} is calculated from Eq. (21) using an average nanoparticle radius $r_M = 4$ nm and a relative dielectric constant of the linker molecules $\epsilon_r = 2.2$ which is typical for hydrocarbons.[25] The void fraction of the nanoparticle films is assumed to be $f_v = 0.3$. Four different combinations of wide and narrow distributions P_λ and P_ϵ are shown where the $\Delta\lambda$ values are $(\Delta\lambda)_1 = 0.1\ \lambda_M$, $(\Delta\lambda)_2 = 2\ \lambda_M$ and $\Delta\epsilon$ values $(\Delta\epsilon)_1 = 0.1\ \epsilon_M$, $(\Delta\epsilon)_2 = 2\ \epsilon_M$. The labeling of the curves in Fig. 3 is as follows: $1 \equiv [(\Delta\lambda)_2, (\Delta\epsilon)_2]$, $2 \equiv [(\Delta\lambda)_2, (\Delta\epsilon)_1]$, $3 \equiv [(\Delta\lambda)_1, (\Delta\epsilon)_2]$, $4 \equiv [(\Delta\lambda)_1, (\Delta\epsilon)_1]$. As can be seen from Fig. 3, wide P_λ and P_ϵ distributions, i.e., $\Delta\lambda = 2\lambda_M$ and $\Delta\epsilon = 2\epsilon_M$, lead to an approximate $\xi_c \sim T^{-\gamma}$ behavior with $\gamma \simeq 0.5$. In contrast, narrow P_ϵ distributions ($\Delta\epsilon = 0.1\epsilon_M$) and narrow P_λ distributions ($\Delta\lambda = 0.1\lambda_M$) show Arrhenius-like behavior, i.e., $\gamma \simeq 1$. It should be noted that in case 3 where the P_λ distribution is narrow but the P_ϵ distribution is wide Arrhenius-like behavior also results. Therefore, in order to observe $\gamma \simeq 0.5$, both P_λ and P_ϵ have to be wide distributions.

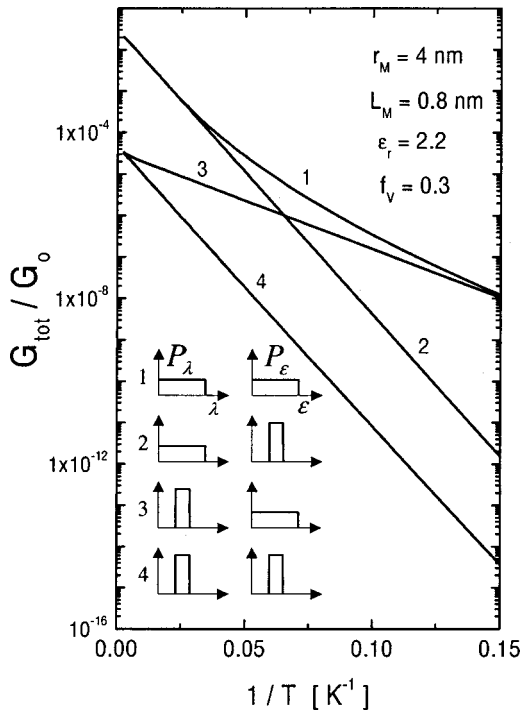

FIG. 3. Calculated film conductance G_{tot} versus $1/T$ for different combinations of $\Delta\lambda$ and $\Delta\epsilon$ using the analytical expression Eq. (24). The labels on the curves are: $1\equiv[(\Delta\lambda)_2,(\Delta\epsilon)_2]$, $2\equiv[(\Delta\lambda)_2,(\Delta\epsilon)_1]$, $3\equiv[(\Delta\lambda)_1,(\Delta\epsilon)_2]$, and $4\equiv[(\Delta\lambda)_1,(\Delta\epsilon)_1]$, where $(\Delta\lambda)_1=0.1\ \lambda_M$, $(\Delta\lambda)_2=2\ \lambda_M$ and $(\Delta\epsilon)_1=0.1\ \epsilon_M$, $(\Delta\epsilon)_2=2\ \epsilon_M$.

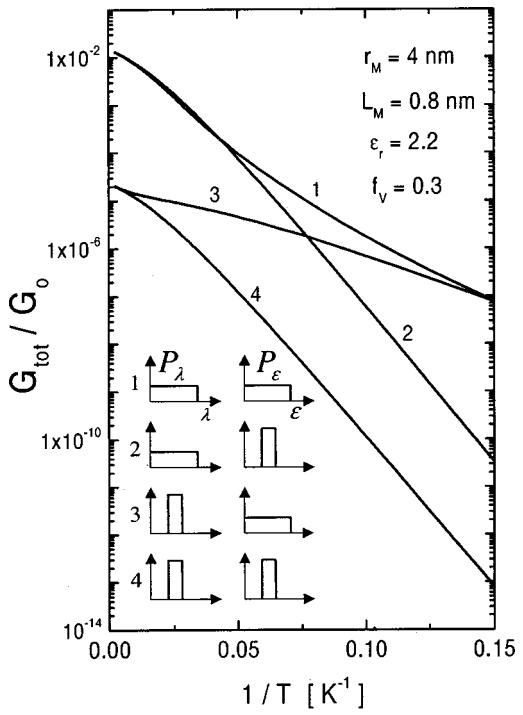

FIG. 4. Calculated film conductance G_{tot} versus $1/T$ for different combinations of $\Delta\lambda$ and $\Delta\epsilon$ using the nonapproximate expression (11) and solving Eq. (18) together with Eqs. (19) and (20). The labels on the curves are those of Fig. 3.

Figure 4 displays the calculated values of $G_{\mathrm{tot}}/G_0=e^{-\xi_c}$ versus $1/T$ for different choices of $\Delta\lambda$ and $\Delta\epsilon$ using the nonapproximate full expression for $g(E_c/kT)$ given by Eq. (11). $\xi_c(T)$ was calculated numerically using Eq. (18) together with Eqs. (11), (19), and (20). Figure 4 is similar to Fig. 3 but deviates in the high temperature range. Because the temperature dependence of ξ_c for a narrow P_ϵ distribution is that of $g(E_c/kT)$ [Eq. (11)], the curves 2, 3 and 4 in Fig. 4 are no longer Arrhenius-like.

Figure 5 shows a comparison between our experimental data for G_{tot} and our calculation using the full expression for $g(E_c/kT)$ of Eq. (11) and numerically solving Eq. (18) using Eqs. (19) and (20). The assembled films consist of Au nanoparticles of average radius $r_M=4$ nm surrounded by alkane dithiol molecules $[\mathrm{HS(CH_2)}_n\mathrm{SH}]$ with $n=2$ and $n=8$. The conductance was measured as a function of temperature T between 5 and 300 K. Because the theory outlined above does not predict the prefactor G_0 in Eq. (14), G_0 was obtained by fitting. The data points used to determine G_0 are indicated in Fig. 5. Excellent agreement between the theory and experimental data is obtained by assuming that the width of the P_ϵ distribution is $\Delta E_c=2E_{cM}$ and that for $n=2$ the width of the P_λ distribution is $\Delta L=1.1L_M$ while for $n=8$, $\Delta L=0.4L_M$. Values for L_M were obtained by estimating the thickness of a self-assembled monolayer of alkane dithiol molecules connecting opposing facets of two gold nanoparticles. For $n=2$, we estimate $L_M=0.8$ nm and for $n=8$,

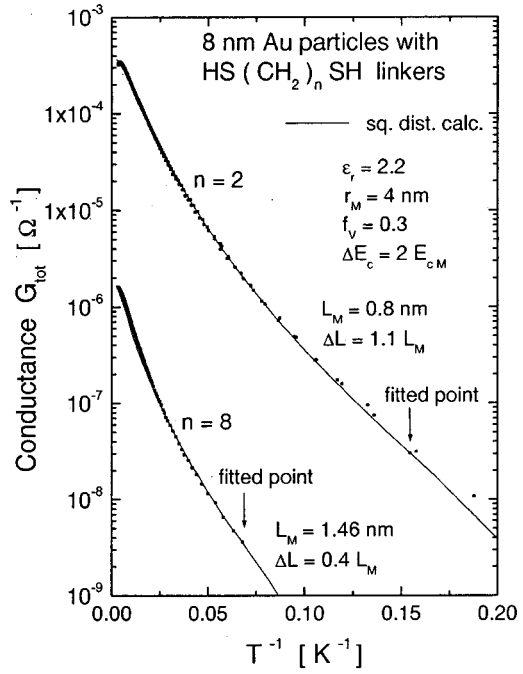

FIG. 5. Calculated and measured values of G_{tot} versus $1/T$ for two films of nanoparticles of radius 4 nm. The linker molecules are $\mathrm{HS(CH_2)}_n\mathrm{SH}$ with $n=2$ and $n=8$. The calculation uses Eq. (18) together with Eqs. (11), (19), and (20).

$L_M = 1.46$ nm.[1] The void fraction of our nanoparticle films was estimated to be $f_v = 0.3$.

V. JUSTIFICATION FOR CHOICE OF P_λ AND P_ϵ DISTRIBUTIONS

As we saw in Fig. 5, assuming a wide P_ϵ distribution and a relatively wide P_λ distribution leads to good agreement with our experimental data. In the following, we estimate the width of the P_λ and P_ϵ distributions in our nanoparticle films.

In the case of the P_λ distribution, if we assume that the nanoparticles in our films vary in size according to a Gaussian distribution and that the organic molecules between the nanoparticles can partially accommodate strain, then the nanoparticle separation L can be expected also to vary according to a Gaussian distribution and $\Delta L \simeq \sqrt{2}\Delta r$, where ΔL and Δr are the full width half maximum (FWHM) values of the nanoparticle separation and size distributions, respectively. Because $\Delta L/L_M = \sqrt{2}(r_M/L_M)\Delta r/r_M$ and because, in our case, $r_M/L_M \gg 1$, a relatively narrow nanoparticle size distribution can cause a wide P_λ distribution.

In the case of the P_ϵ distribution, the width of the charging energy distribution P_ϵ is determined by the degree of nanoparticle size variation as well as by possible random offset charges. To evaluate the Coulomb charging energy E_c we use the general expression for the electrostatic energy F of a capacitively coupled system of two neighboring nanoparticles,[26] i.e.,

$$F = \frac{1}{2}\sum_{i,j=1}^{2} Q_i (C_{ij})^{-1} Q_j. \tag{28}$$

Here Q_i is the charge on nanoparticle $i = 1,2$ and $(C_{ij})^{-1}$ is the inverse capacitance matrix, where the electrostatically interacting pair of neighboring nanoparticles is thought to be embedded in an effective medium of permittivity ϵ_{eff} generated by the surrounding nanoparticles. The Coulomb charging energy is given by $E_c = \Delta F$ where ΔF is the change in electrostatic energy when an electron tunnels from one nanoparticle to a neighboring one, i.e., when $(Q_1 = 0,\ Q_2 = 0)$ changes to $(Q_1 = -e,\ Q_2 = +e)$. We obtain

$$E_c = \frac{e^2}{2}\frac{C_{11} + 2C_{12} + C_{22}}{C_{11}C_{22} - C_{12}^2}. \tag{29}$$

Employing the method of image charges one derives[27]

$$C_{11} = 4\pi\epsilon_0\epsilon_{\text{eff}} r_1 r_2 \sinh(\alpha)\sum_{n=1}^{\infty}\{r_2\sinh(n\alpha) + r_1\sinh[(n-1)\alpha]\}^{-1}, \tag{30}$$

$$C_{22} = 4\pi\epsilon_0\epsilon_{\text{eff}} r_1 r_2 \sinh(\alpha)\sum_{n=1}^{\infty}\{r_1\sinh(n\alpha) + r_2\sinh[(n-1)\alpha]\}^{-1}, \tag{31}$$

and

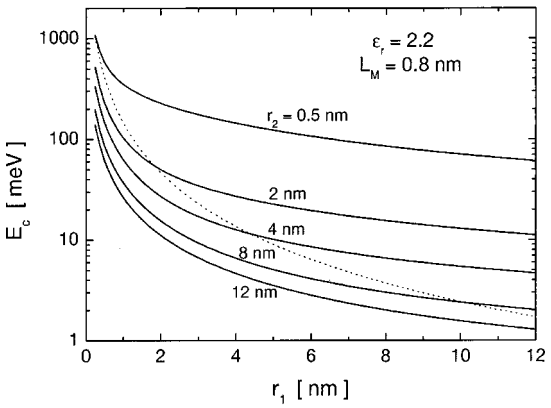

FIG. 6. Charging energy E_c versus radius r_1 of particle 1 for different radii r_2 of the neighboring particle 2. The dashed line represents Eq. (21) with $r_M = r_1$.

$$C_{12} = 4\pi\epsilon_0\epsilon_{\text{eff}}\frac{r_1 r_2}{d}\sinh(\alpha)\sum_{n=1}^{\infty}[\sinh(n\alpha)]^{-1}. \tag{32}$$

Here r_1 and r_2 are the radii of the two neighboring nanoparticles and

$$\cosh\alpha = \frac{d^2 - r_1^2 - r_2^2}{2r_1 r_2} \tag{33}$$

with

$$d = r_1 + r_2 + L. \tag{34}$$

The effective permittivity due to the surrounding nanoparticles is estimated to be

$$\epsilon_{\text{eff}} = \left(1 + \frac{r_1 + r_2}{2L_M}\right)\epsilon_r. \tag{35}$$

In order to derive the above expression for ϵ_{eff}, a nanoparticle and its surroundings were modeled by a nanoparticle surrounded by a dielectric shell of thickness L_M and dielectric constant ϵ_r embedded in an infinite homogeneous metal.[11]

Figure 6 shows the Coulomb charging energy E_c versus radius r_1 of particle 1 for different radii r_2 of particle 2 using $L = L_M = 0.8$ nm and $\epsilon_r = 2.2$. The charging energy increases rapidly when r_1 and r_2 decrease. The dashed line shows E_c using the Abeles formula [Eq. (21)] with $r_M = r_1 = r_2$.

Assuming a Gaussian nanoparticle size distribution, we have calculated numerically using Eqs. (29)–(35) the probability density $P_\epsilon(E_c)$. The result is shown in Fig. 7. The width of the P_ϵ distribution increases in a similar way to the underlying particle size distribution but is skewed towards lower E_c values for larger $\Delta r/r_M$. These calculations indicate that a narrow nanoparticle size distribution leads to a narrow distribution of charging energies.

A significant broadening of the P_ϵ distribution occurs when offset charge disorder is present. Offset charge disorder

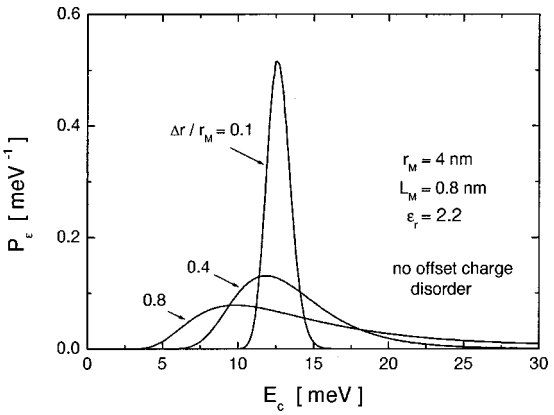

FIG. 7. Calculated probability density P_ϵ versus the Coulomb charging energy E_c for different choices of the FWHM value Δr of the assumed Gaussian nanoparticle size distribution. Offset charge disorder was not considered.

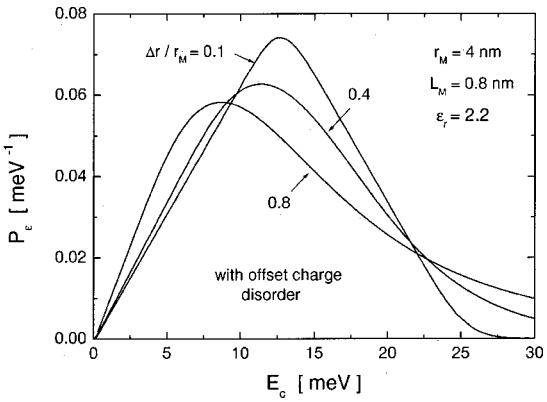

FIG. 8. Calculated probability density P_ϵ versus Coulomb charging energy E_c for different choices of the FWHM value Δr of the assumed Gaussian nanoparticle size distribution. Maximal random offset charge disorder is assumed.

is caused by charges trapped in the substrate or in the linker molecules which induce fractional charges on the metal nanoparticles. Denoting by q_1 and q_2 the induced charges on neighboring particles 1 and 2, we derive using Eq. (28)

$$E_c=\frac{e^2}{2}\frac{(1-2q_2)C_{11}+2(q_2-q_1-1)C_{12}+(2q_1+1)C_{22}}{C_{11}C_{22}-C_{12}^2}, \tag{36}$$

where C_{11}, C_{22}, and C_{12} are given by Eqs. (30)–(32). Assuming a Gaussian nanoparticle size distribution we have calculated numerically, using Eq. (36), the probability density P_ϵ assuming maximal offset charge disorder, i.e., $-0.5e \leqslant q_{1/2} \leqslant 0.5e$ with constant probability.[4] Figure 8 shows that for $r_M=4$ nm, $L=L_M=0.8$ nm, and $\epsilon_r=2.2$ wide, triangular-shaped P_ϵ distributions result which are only slightly dependent on the relative width $\Delta r/r_M$ of the Gaussian nanoparticle size distribution. For $\Delta r/r_M \to 0$ (monoparticle size distribution), P_ϵ becomes exactly triangular in shape and has a width of E_{cM}. Because the average separation gap around a nanoparticle fluctuates locally around its mean value L_M, a further broadening of P_ϵ can be expected. It should be noted that α in Eq. (33) depends on L via Eq. (34), and thus E_c and L are correlated. Because in our case $L \ll r_{1/2}$, this correlation is weak and could be neglected when expressing $P(\xi)$ in Eq. (16) as an integral over the product of probability densities P_λ and P_ϵ.

VI. CONCLUSION

We have investigated experimentally and theoretically the temperature dependence of the electron conduction in disordered Au nanoparticle films linked by alkane dithiol molecules in the temperature range from 5 to 300 K for small applied voltages. Electron transport between nanoparticles is described theoretically using scattering theory between two Fermi gases representing the electrons in adjacent nanoparticles, while the effect of the organic linker molecules can be approximated in terms of a tight binding model. Local disorder in our films is caused by particle size variations and fluctuations in the separation gap between adjacent nanoparticles as well as by random immobile offset charges induced by trapped impurity charges in the substrate and possibly in the linker molecules. Because of this disorder, the local tunnel conductances between adjacent nanoparticles vary over several orders of magnitude which allows us to employ percolation theory to estimate the temperature dependence of the conductance $G_{\rm tot}$ of the film. Experimentally, we find a non-Arrhenius temperature dependence for the conductance where $\ln(G_{\rm tot}/G_0) \sim T^{-1/2}$. Our percolation theory approach can predict non-Arrhenius behavior as electrons are able to select different percolation paths at different temperatures which leads to an enhanced conductance at low temperatures. We find that in order to describe our experimental results accurately, wide distributions of Coulomb charging energies and nanoparticle separation gaps are needed. Our calculations have shown that a wide Coulomb charging energy distribution can be expected from the presence of random offset charges even if the nanoparticle size distribution is narrow.

*Electronic address: karl.muller@csiro.au

[1] N. Fishelson, I. Shkrob, O. Lev, J. Gun, and A. Modestov, Langmuir **17**, 403 (2001).

[2] R. H. Terrill, T. A. Postlethwaite, C. Chen, C.-D. Poon, A. Terzis, A. Chen, J. E. Hutchison, M. R. Clark, G. Wignall, J. D. Londono, R. Superfine, M. Falvo, C. S. Johnson Jr., E. T. Samulski, and R. W. Murray, J. Am. Chem. Soc. **117**, 12 537 (1995).

[3] C. P. Collier, T. Vossmeyer, and J. R. Heath, Annu. Rev. Phys. Chem. **49**, 371 (1998).

[4] A. A. Middleton and N. S. Wingreen, Phys. Rev. Lett. **71**, 3198 (1993).

[5] A. S. Cordan, A. Goltzené, Y. Hervé, M. Mejias, C. Vieu, and H. Launois, J. Appl. Phys. **84**, 3756 (1998).

[6] H.-O. Müller, K. Katayama, and H. Mizuta, J. Appl. Phys. **84**, 5603 (1998).

[7] A. S. Cordan, Y. Leroy, A. Goltzené, A. Pépin, C. Vieu, M. Me-

jias, and H. Launois, J. Appl. Phys. **87**, 345 (2000).
[8] J. Johansson and D. B. Haviland, Phys. Rev. B **63**, 014201 (2000).
[9] A. Messiah, *Quantum Mechanics* (North-Holland, Amsterdam, 1970), Vol. 2.
[10] J. Lambe and R. C. Jaklevic, Phys. Rev. **165**, 821 (1968).
[11] K. K. Likharev, Proc. IEEE **87**, 606 (1999).
[12] V. Mujica, M. Kemp, and M. A. Ratner, J. Chem. Phys. **101**, 6856 (1994).
[13] A. Onipko, Y. Klymenko, L. Malysheva, and S. Stafström, Solid State Commun. **108**, 555 (1998).
[14] D. J. Wold and C. D. Frisbie, J. Am. Chem. Soc. **122**, 2970 (2000).
[15] R. E. Holmlin, R. Haag, M. L. Chabinyc, R. F. Ismagilov, A. E. Cohen, A. Terfort, M. A. Rampi, and G. M. Whitesides, J. Am. Chem. Soc. **123**, 5075 (2001).
[16] V. Ambegaokar, B. I. Halperin, and J. S. Langer, Phys. Rev. B **4**, 2612 (1970).
[17] M. Pollak, J. Non-Cryst. Solids **11**, 1 (1972).
[18] B. I. Shklovskii and A. L. Efros, *Electronic Properties of Doped Semiconductors*, Vol. 45 of *Springer Series in Solid-State Sciences* (Springer-Verlag, Berlin, 1984).
[19] M. B. Isichenko, Rev. Mod. Phys. **64**, 961 (1992).
[20] B. Abeles, P. Sheng, M. D. Coutts, and Y. Arie, Adv. Phys. **24**, 407 (1975).
[21] B. Raguse, J. Herrmann, G. Stevens, J. Myers, G. Baxter, K.-H. Müller, T. Reda, A. Molodyk, and V. Braach-Maksvytis, J. Nanoparticle Res. (to be published).
[22] M. Brust, M. Walker, D. Bethell, D. J. Schiffrin, and R. Whyman, J. Chem. Soc. Chem. Commun. **7**, 801 (1994).
[23] M. Brust, D. Bethell, D. J. Schiffrin, and C. J. Kiely, Adv. Mater. **7**, 795 (1995).
[24] Durapore membrane filter, 0.22 μm nominal filter pore size, Millipore Co.
[25] *CRC Handbook of Chemistry and Physics*, edited by D. R. Lide (CRC Press, Boca Raton, 1994), 75th ed.
[26] L. D. Landau and E. M. Lifshitz, *Electrodynamics of Continuous Media* (Pergamon Press, Oxford, 1993).
[27] W. R. Smythe, *Static and Dynamic Electricity* (McGraw-Hill, New York, 1939).